Available online at www.sciencedirect.com

ScienceDirect

Procedia Engineering 205 (2017) 1004–1010

Procedia Engineering

www.elsevier.com/locate/procedia

10th International Symposium on Heating, Ventilation and Air Conditioning, ISHVAC2017, 19-22 October 2017, Jinan, China

Pedestrian Level Turbulent Wind Flow around an Elevated Building

Jianlin Liu[a, b, *], Jianlei Niu[a, c], Cheuk Ming Mak[a] and Qian Xia[a]

[a]*Department of Building Services Engineering, The Hong Kong Polytechnic University, Hung Hom, Kowloon, Hong Kong*
[b]*State Key Laboratory of Subtropical Building Science of South China University of Technology, Guangzhou, China*
[c]*School of Architecture, Design and Planning, The University of Sydney, Sydney, Australia*

Abstract

Wind flow turbulence plays a critical role in the pedestrian level wind environment, particularly for the airflow around buildings with specific architectural features. The elevated design, a feature was proved to improve the pedestrian level weak wind conditions in high-density cities in our earlier study. This present study aims to further investigate the pedestrian level wind flow turbulence in an elevated building surrounding. The predictions were conducted by comparing the CFD simulation and a wind tunnel experiment. Specifically, the Detached Eddy Simulation (DES), the Steady-state and the Unsteady-state RANS (SRANS and URANS), were assessed. The effects of mesh resolutions and inflow fluctuating algorithms on the performance of the DES model were thoroughly evaluated. DES can better reproduce the mean flow fields than the other two models. The unsteady flow fluctuations around the elevated building are analyzed with energy spectral density. Meanwhile, the periodical wind flow fields around the elevated building are accurately obtained.

Peer-review under responsibility of the scientific committee of the 10th International Symposium on Heating, Ventilation and Air Conditioning.

Keywords: CFD simulation, Pedestrian level wind (PLW), DES (Detached eddy simulation), Unsteady-state RANS (URANS), Elevated building;

1. Introduction

The outdoor wind/thermal comfort in cities are significant for they are correlating to people's outdoor living conditions and recreational activities [1, 2]. Some architectural features modify the wind flow conditions in building surroundings at the pedestrian level. The building elevated design (lift-up), a frequently used feature in Asia subtropical cities, would form an open space underneath an elevated building that may function as a corridor for

* Corresponding author. Tel.: +852-276-678-01; fax: +852-276-571-98.
E-mail address: jian-lin.liu@connect.polyu.hk

1877-7058
Peer-review under responsibility of the scientific committee of the 10th International Symposium on Heating, Ventilation and Air Conditioning.
10.1016/j.proeng.2017.10.160

wind [2]. In particular, the open space underneath an elevated building was more favorable and more thermally comfortable on a hot summer day [2, 3]. In the recent studies [3-5], the ground pedestrian-level aerodynamics of several elevated building blocks were investigated via wind tunnel testing and CFD simulation. The area underneath the elevated building was found to have a higher wind amplification ratio than that of the building surrounding. However, limited turbulent flow fluctuations were focused on the flow around the elevated building. For the planning stage, the planners desire to know the modification of the instantaneous Pedestrian level wind (PLW) flow field if this design would be utilized.

PLW flow around buildings is mainly analyzed by three methods, including on-site measurement, wind tunnel test, and Computational Fluid Dynamics (CFD) simulation, while the former two in the PLW flow are time-consuming in the setup and measurement steps [6]. CFD is avoiding this problem to obtain the entire image of the flow field. For the turbulence models in the core of CFD, a hybrid URANS/LES modeling approach, termed the Detached Eddy Simulation (DES), was proposed to alleviate the computing time-consuming problem between pure RANS and pure LES, and was first used by Spalart et al. [7] to simulate the air flow around an airfoil. More recently, the effects of the physical and numerical parameters, such as mesh resolution, discretized time step size and sampling time by DES was assessed by Liu and Niu [8] on the flow around a single building and indicated that DES could provide similar performances as those of LES but with lower mesh numbers and computing time requirements. In the transient simulation of wind flow in outdoor built environment, a significant issue is the setup of inflow fluctuating boundary conditions at the computational domain inlet. The inflow conditions of the LES and DES require varying randomly, while they must be compatible with the N–S equations [9].

2. Methods

2.1. Turbulence model

The hybrid modeling approach, DES, modified the standard formulation of S-A turbulence model [7] into the unsteady mode and revised the length scale d by a new variable $\tilde{d}$, $\tilde{d} = \min(d, C_{des}\Delta)$, where the filter size Δ is the largest grid space in the x, y, or z directions of the grid cell ($\Delta = \max(\Delta x, \Delta y, \Delta z)$) and the additional empirical value C_{des} is 0.65 [8]. The defined $\tilde{d}$ ensures the switching behavior of DES between URANS and LES modes. The LES mode is applied if $d > \Delta$, and the URANS mode is used if $d < \Delta$. Spalart, Deck, Shur, Squires, Strelets and Travin [10] further improved the standard DES [7] to the DDES model to solve this problem and obtain a more precise delineation of the boundary layer. This model preserved the URANS mode or delayed the LES mode in the boundary layer. The DDES model is used in this study based on the above discussion and the authors' earlier assessing studies among different turbulence models, including SRANS, LES and DES [8].

2.2. Simulation setup and numerical method

The wind tunnel experiment was conducted by Xia et al. [4] of the wind flow around an isolated building with an elevated design. The single building had dimensions of 25 m (D) × 75 m (W) × 50 m (H) at the prototype scale for the streamwise x, lateral y, and vertical z directions, respectively. The elevated design was added with three structural pillars and each with the size in prototype was set as 8 m × 8 m × 3.5 m (h). The building model was constructed on a geometric scale of 1:200 and placed in the wind tunnel (Fig. 1). The wind inflow profile was presented as the normalized mean streamwise velocity and the turbulence intensity was $I(z)$, where the reference mean wind velocity, u_r was 10 m/s at the approaching flow of the reference height at the prototype scale z_r = 150 m (0.75 m at the model scale). The measurement points (in Figure.1(c)) at the normalized height of z/H = 0.04 are used here for CFD validation. Notably, the measured mean wind velocity u_{xy} has no direction at the horizontal plane in the wind tunnel test.

The size of the computational domain was 13.5H × 11.5H × 6H for the length, width, and height, respectively. The width and the height of the domain were set as the recommended values of Tominaga et al. [11]. The length of building windward was slightly set below the recommended values to reduce the deterioration of the prescribed inflow profiles along upstream of the building [12]. The resulting blockage ratio of this set of domain size was 2.2%. The computational domain was discretized with hexahedral grids (Fig. 2). According to the mesh arrangement

method for DES by Liu and Niu [8] , different grid spacings were required for the windward side (Euler and RANS regions), lateral sides, and leeward side (LES region) of the air flow around a bluff body. The mesh arrangements were illustrated in Table 1 for the RANS (included SRANS and URANS) and DES cases, such as mesh numbers, Courant-Friedrichs-Lewy (CFL) number, computing time and mean non-dimensional wall distance y^+ values.

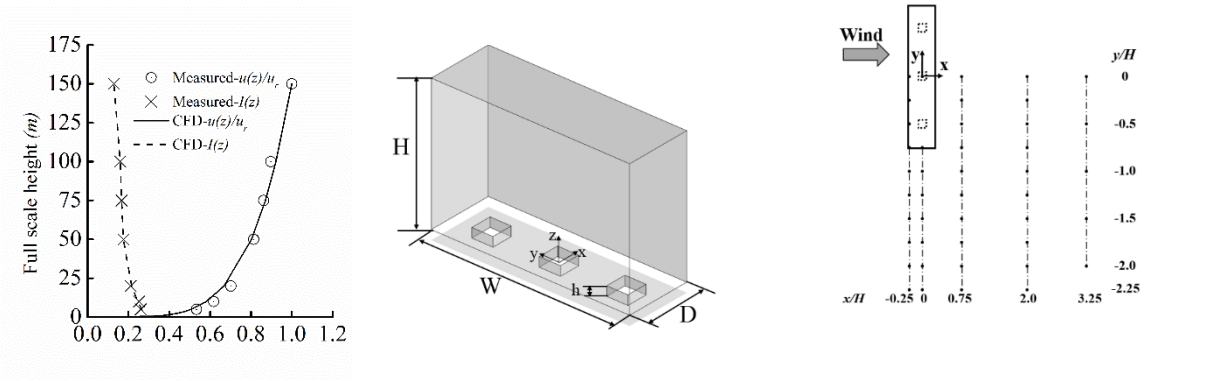

Fig. 1. Wind inflow profile and the building configurations: (a) wind profile of streamwise wind velocity and turbulence intensity, (b) single elevated building [3] and (c) measurement points at the pedestrian level

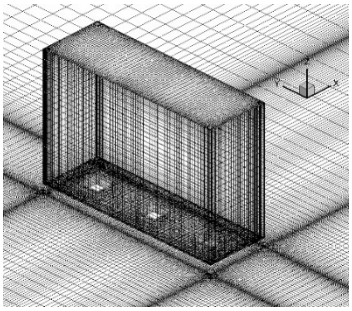

Fig. 2. Mesh information: 3-dimensional view of DES-lift-2

Table 1. Mesh arranged descriptions and computing time costs of RANS and DES cases

Case	Mesh numbers (million)	Min grid size (m)	Turbulence model	CFL	Δt (s)	t^*	y^+	Computing time (h)
RNG-lift	2.80	0.001	RNG k-ε	-	-	-	4.85	7.2
URANS-lift	2.80	0.001	RNG k-ε	1.75	0.005	448	4.85	69.4
DES-lift-1	2.80	0.001	DDES	1.48	0.005	288	4.85	32.2
DES-lift-2	3.54	0.0005	DDES	1.42	0.005	288	2.53	76.8
DES-lift-3	5.66	0.00025	DDES	0.92	0.005	288	1.58	129.6

The flow fields of the converged SRANS simulations were used as the initial conditions for the URANS and DES cases. The inlet profile of domain boundary was imposed on the vertical inflow profile of mean velocity and the turbulence intensity of Xia et al. [4]. The turbulent kinetic energy k (= $1.5(I(z)u(z))^2$) and its dissipation rate ε (= $C_\mu^{0.5}\, k\, du/dz$, $C_\mu = 0.09$) were calculated with the assuming local equilibrium of $P_k = \varepsilon$. The commercial code Fluent 13.0 provides three inflow fluctuating algorithms for the DDES models but not in the unsteady-state RNG k–ε model, including No perturbations, Vortex method, and Spectral Synthesizer. The lateral and top boundaries of the domain were set to have no vertical gradients for any of the parameters as with the validation case [8]. The ground and building surfaces were defined as no-slip condition walls. All simulations were calculated until the residuals were below 10^{-4} for continuity and 10^{-6} for velocity, k and ε. In RANS cases, the discretized equations were solved by SIMPLEC algorithm, while the convection and diffusion terms were discretized by the second-order up wind scheme. In the DES simulation, the PISO algorithm was selected, and the bounded central differencing and the

second-order upwind scheme were utilized for the convective terms and the diffusion terms, respectively. The second-order implicit scheme was used for the temporal discretization. The discretized time step (Δt = 0.005 s) and the non-dimensional sampling time length ($t^* = t \times u_H/H$ = 288, which is equal to a real period t of 9 s in this study) were selected to obtain the mean statistical values based on the influence tests of Δt and t^* by Liu and Niu [8].

3. Results

3.1. Effect of mesh resolution

The simulated results with building elevation for the DES-lift-1 demonstrate more differences than the other two cases, particularly in Fig. 3(b). The results for the DES-lift-2 are approximately the same with the DES-lift-3. However, Fig. 3(c) shows that a coarse mesh has a more similar performance to the fine mesh than the medium one. The possible factor is that the inconsistent relationships among the mesh resolution and accuracy of results in transient simulations [13]. The computing time increase with the mesh numbers, where the times are 32.2, 76.8, and 129.6 h for DES-lift-1, 2, and 3, respectively. Consequently, the mesh number of DES-lift-2 are the economical choice which saves the computing time for our study under the present hardware conditions.

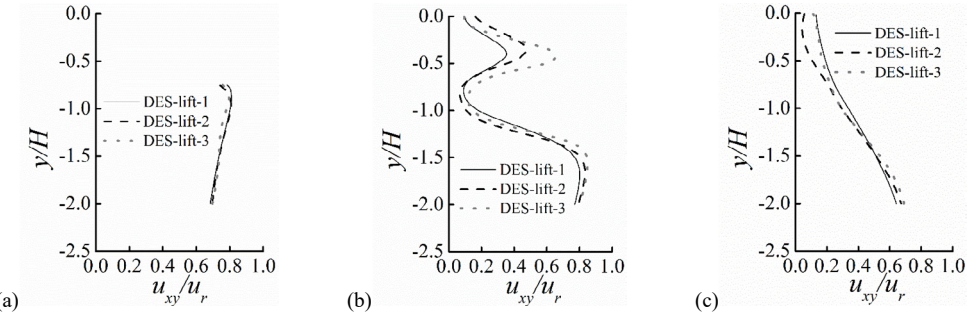

Fig. 3. The mean wind velocity distribution around a single elevated for coarse, medium, and fine DDES cases: (a) x/H = −0.25, (b) x/H = 0.75 and (c) x/H = 3.25

3.2. Effect of inflow fluctuating algorithm on DDES

Three sorts of inflow fluctuating algorithms are frequently used in outdoor wind simulations. The first method, no perturbations (NP), ignores the inflow fluctuating components and only the streamwise wind velocity profile is embedded in the inlet of the computational domain. The other algorithm, the vortex method (VM), has been used by some LES practitioners. The vortex method inserts the perturbations into the mean flow velocity profile by randomly transporting certain numbers of 2D vortices on the computational domain inlet. The third method, the spectral synthesizer (SS), generates the fluctuating velocity components by randomly synthesizing a divergence-free velocity field from the summation of the Fourier harmonics. Fig. 4 presents the effect of the inflow fluctuating algorithm on the DDES performance of the wind flow around a single building. Results indicate that the case VM shows similar results on the predicted velocity field as the experiment does. The velocity distributions provided by NP and SS are similar, and their results deviated from the wind tunnel data in some areas, particularly near the building facade at y/H = 0 to −0.8 in Fig. 4(b). Because the perturbations imposed on the inlet wind velocity profile are lower or nonexistent, NP and SS provide an underestimated wind velocity near the building lateral side and the wake region. Consequently, the VM algorithm shows a better performance than the other two when using the DDES model in the wind flow around a single building.

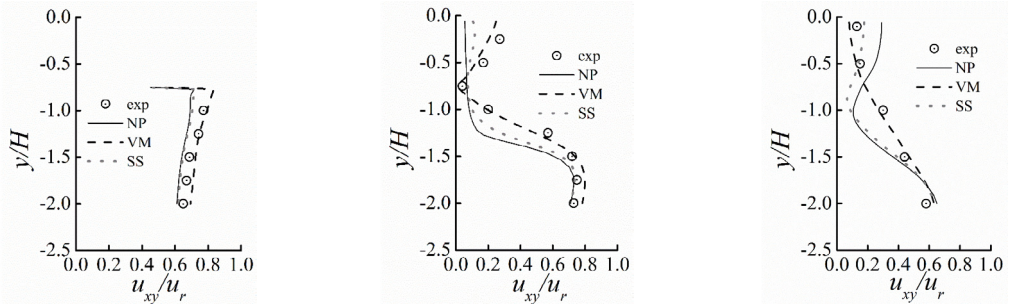

(a) x/H= −0.25 (b) x/H= 0.75 (c) x/H= 3.25

Fig. 4. Comparison of inflow fluctuations on the mean wind velocity distributions

3.3. Validations of SRANS, URANS and DDES

Fig. 5 demonstrates the normalized mean velocity distributions for the elevated building. Different flow characteristics show near the building leeward facade with the added elevated building design at x/H = 0.75. Specifically, DES-lift presents a better performance on the shapes of curves at the building leeward side of y/H = 0 to −0.7 in accordance with the experiment at x/H = 0.75, while the two RANS cases underestimate the wind velocity at this region; but they overestimate it at x/H = 2.0 even when the transient simulation is used by URANS case. The URANS-lift presents more differences from the Steady-state RNG-lift and DES-lift, and overestimates the wind velocity at y/H = 0 to −0.5 and −1.5 to 2.0 at the measurement line of x/H = 3.25. As a result, the performance of URANS is not better than that of the SRANS in the mean flow prediction around a single building with the elevated design, particularly in the building wake region, while the URANS simulation requires more computing time (Table 1) than the steady-state RNG simulation even if the same mesh resolution is used. Therefore, the DDES model demonstrates a better performance than the both SRANS and URANS in the obtained mean flow field around a single building with elevation.

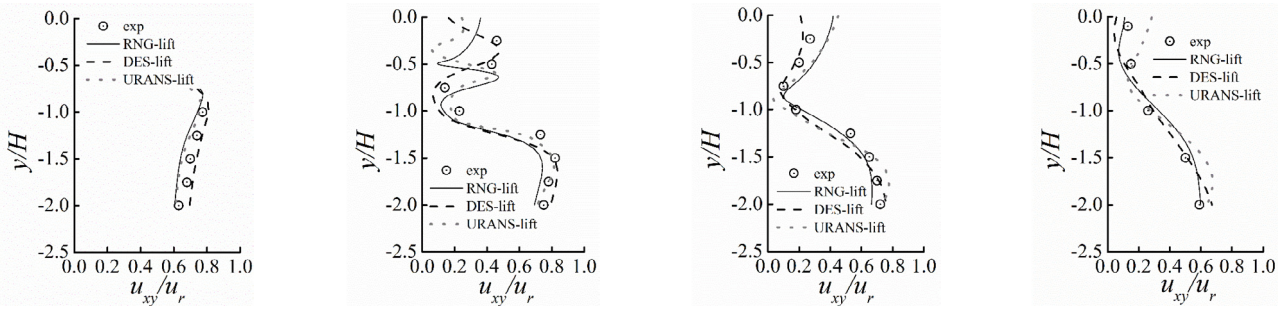

(a) (b) (c) (d)

Fig. 5. Normalized mean velocity distributions for the single elevated building: (a) x/H = −0.25, (b) x/H = 0.75, (c) x/H = 2.0, and (d) x/H = 3.25

3.4. Unsteady flow fluctuations produced by DES modeling

The DDES simulation can provide the instantaneous wind flow results. Further analysis of unsteady flow fluctuations with Energy Spectral Density (ESD) of the turbulent flow. The time histories of velocity u/u_r were monitored downstream of the building for the case DES-lift-2 (with elevation). Three discrete monitored points 1, 2 and 3 of non-dimensional coordinates x/H = 1, 2 and 3 are set at the same line y/H = −0.75, z/H = 0.04. The fluctuations of velocity components for each point are clearly observed. Fig. 6 shows the ESD of the fluctuating velocity at three monitored points and the lift coefficient C_L for the building with the elevated design. *St* here is defined as $St = n \times W/u_h$ (n is the frequency, Hz). The peak *St* at the coordinate x signifies that this value would be distinguished as the dominant vortex shedding frequency. The *St* of the vortex shedding behind building with the elevated design ranges of 0.08 – 0.13. The obtained *St* are consistent with the reported value of a single building in

the literature [14]. Therefore, the DDES model is accurate in predicting the frequency in the wake region of the building with the elevated design. The period T (=$1/n$) of vortex shedding represents the time which takes for a vortex to complete the formation at a surface, following the separation and shedding from the building until the new one starts to form. The calculated non-dimensional time length for one vortex shedding period are 16.6 with using the St of C_L, 0.09 for the elevated building.

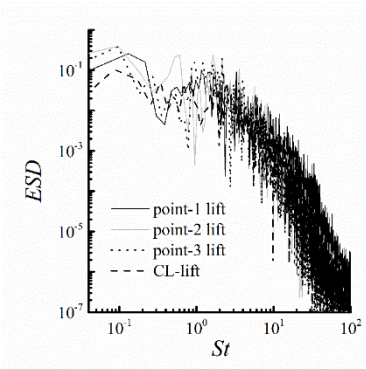

Fig. 6. ESD of the velocity fluctuations at monitored points and the lift coefficient for the elevated building

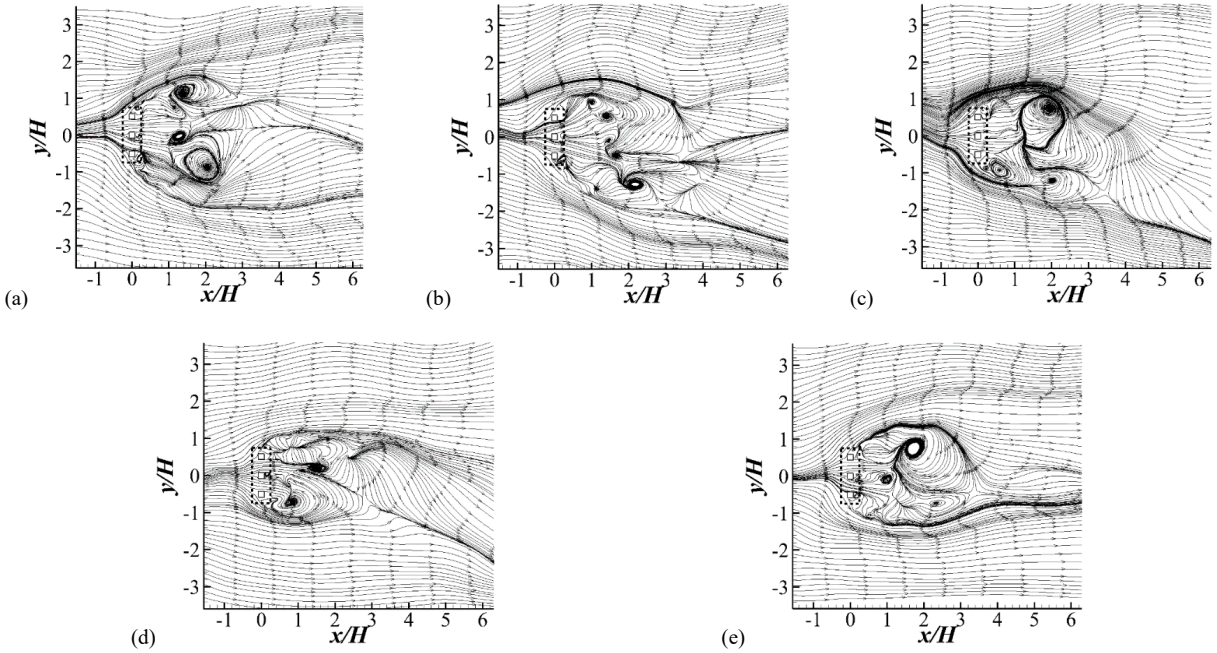

Fig. 7. Instantaneous wind streamlines for flow around the building with elevation on the X–Y plane: (a) at time t, (b) at t + T/4, (c) at t + T/2, (d) at t + 3T/4, and (e) at t + T

The instantaneous flow patterns obtained by the DDES model are complex and irregular in Fig. 7 for the elevated building. Wind flow can freely blow through the open space underneath the elevated building block. Small vortices are produced behind each structural pillar. Many vortices forms and sheds at high frequency in the wake region of the elevated building block. The numbers of pairs of vortices are increased behind the building, while the main pair of vortices is less apparent. The non-dimensional time length of a vortex shedding period is roughly 16.0 for the airflow around the elevated building, which is consistent with the result of the ESD analysis. The reproduced complicated wind flow pattern by DDES model is substantially modified by the elevated design, which can possibly lead to more local areas with different wind conditions during the pedestrian level wind comfort assessments.

4. Conclusions

The findings are summarized as follows: (a) The effect of mesh resolution on the DDES model for the flow around an elevated building is thoroughly tested, the recommended y^+ is around 2. (b) Vortex Method shows better a performance than the NP and SS inflow fluctuating algorithms by the DDES model in the wind flow around a single building. (c) The results of DDES are more consistent with the mean experimental results than those of the SRANS and URANS predictions. (d) Periodically instantaneous flow patterns around a building with the elevated design can be reasonably obtained by the DDES model. The work reveals that the transient CFD simulation of turbulent wind flow effects can be reasonably obtained with a more sophisticated turbulence model which demonstrates the potentials into outdoor wind environment assessment in urban planning.

Acknowledgements

The work described in this paper was supported by the State Key Laboratory of Subtropical Building Science of South China University of Technology with the project No. 2016ZB04 and a grant from the Research Grants Council of the Hong Kong Special Administrative Region, China (Project No. C5002-14G).

References

[1] B. Blocken, T. Stathopoulos, J.P.A.J. van Beeck, Pedestrian-level wind conditions around buildings: Review of wind-tunnel and CFD techniques and their accuracy for wind comfort assessment, Building and Environment 100 (2016) 50-81.
[2] J. Niu, J. Liu, T.-c. Lee, Z. Lin, C. Mak, K.-T. Tse, B.-s. Tang, K.C.S. Kwok, A new method to assess spatial variations of outdoor thermal comfort: Onsite monitoring results and implications for precinct planning, Building and Environment 91 (2015) 263-270.
[3] J. Liu, J. Niu, Q. Xia, Combining measured thermal parameters and simulated wind velocity to predict outdoor thermal comfort, Building and Environment 105 (2016) 185-197.
[4] Q. Xia, X. Liu, J. Niu, K.C.S. Kwok, Effects of building lift-up design on the wind environment for pedestrians, Indoor and Built Environment 0(0) (2015) 1- 18, http://dx.doi.org/10.1177/1420326X15609967 (in press).
[5] Y. Du, C.M. Mak, J. Liu, Q. Xia, J. Niu, K.C.S. Kwok, Effects of lift-up design on pedestrian level wind comfort in different building configurations under three wind directions, Building and Environment 117 (2017) 84-99.
[6] P. Moonen, T. Defraeye, V. Dorer, B. Blocken, J. Carmeliet, Urban Physics: Effect of the micro-climate on comfort, health and energy demand, Frontiers of Architectural Research 1(3) (2012) 197-228.
[7] P. Spalart, W. Jou, M. Strelets, S. Allmaras, Comments on the feasibility of LES for wings, and on a hybrid RANS/LES approach, in: Proceedings of the first AFOSR international conference on DNS/LES, C. Liu, USA, 1997, pp. 137-147.
[8] J. Liu, J. Niu, CFD simulation of the wind environment around an isolated high-rise building: An evaluation of SRANS, LES and DES models, Building and Environment 96 (2016) 91-106.
[9] G.R. Tabor, M.H. Baba-Ahmadi, Inlet conditions for large eddy simulation: A review, Computers & Fluids 39(4) (2010) 553-567.
[10] P.R. Spalart, S. Deck, M. Shur, K. Squires, M.K. Strelets, A. Travin, A new version of detached-eddy simulation, resistant to ambiguous grid densities, Theoretical and computational fluid dynamics 20(3) (2006) 181-195.
[11] Y. Tominaga, A. Mochida, R. Yoshie, H. Kataoka, T. Nozu, M. Yoshikawa, T. Shirasawa, AIJ guidelines for practical applications of CFD to pedestrian wind environment around buildings, Journal of Wind Engineering and Industrial Aerodynamics 96(10–11) (2008) 1749-1761.
[12] B. Blocken, J. Carmeliet, T. Stathopoulos, CFD evaluation of wind speed conditions in passages between parallel buildings—effect of wall-function roughness modifications for the atmospheric boundary layer flow, Journal of Wind Engineering and Industrial Aerodynamics 95(9–11) (2007) 941-962.
[13] P. Gousseau, B. Blocken, G.J.F. van Heijst, Quality assessment of Large-Eddy Simulation of wind flow around a high-rise building: Validation and solution verification, Computers & Fluids 79 (2013) 120-133.
[14] Y. Tominaga, A. Mochida, S. Murakami, S. Sawaki, Comparison of various revised k–ε models and LES applied to flow around a high-rise building model with 1:1:2 shape placed within the surface boundary layer, Journal of Wind Engineering and Industrial Aerodynamics 96(4) (2008) 389-411.